China Ocean Eng., Vol. 28, No. 5, pp. 645 – 657

DOI 10.1007/s13344-014-0051-2, ISSN 0890-5487

Analysis of EMD Algorithm for Identification and Extraction of An Acoustic Signal in Underwater Channel Against Wind Driven Ambient Noise

S. Sakthivel MURUGAN[a, 1], V. NATARAJAN[b] and K. MAHESWARAN[c]

[a] *ECE Department*, *SSN College of Engineering*, *Chennai*, *India*

[b] *Instrumentation Department*, *MIT Campus*, *Anna University*, *Chennai*, *India*

[c] *Infosys*, *Chennai*, *India*

(Received 11 May 2012; received revised form 2 November 2012; accepted 8 June 2013)

ABSTRACT

Sonar generated acoustic signals transmitted in underwater channel for distant communications are affected by numerous factors like ambient noise, making them nonlinear and non-stationary in nature. In recent years, the application of Empirical Mode Decomposition (EMD) technique to analyze nonlinear and non-stationary signals has gained much attention. It is an empirical approach to decompose a signal into a set of oscillatory modes known as intrinsic mode functions (IMFs). In general, Hilbert transform is used in EMD for the identification of oscillatory signals. In this paper a new EMD algorithm is proposed using FFT to identify and extract the acoustic signals available in the underwater channel that are corrupted due to various ambient noises over a range of 100 Hz to 10 kHz in a shallow water region. Data for analysis are collected at a depth of 5 m and 10 m offshore Chennai at the Bay of Bengal. The algorithm is validated for different sets of known and unknown reference signals. It is observed that the proposed EMD algorithm identifies and extracts the reference signals against various ambient noises. Significant SNR improvement is also achieved for underwater acoustic signals.

Key words: *EMD*; *IMF*; *SNR*; *ambient noises*; *underwater acoustic signals*; *FFT*

1. Introduction

Underwater acoustic communications research is rapidly growing as commercial applications are increasing in this field. When an acoustic signal is transmitted by using water as a channel, apart from various types of losses like reverberation, attenuation, absorption, scattering, and the acoustic signal also undergoes distortion due to ambient noises. Ambient noises in underwater acoustics are the background noises in the ocean. The sources for ambient noises can be either natural (due to rain, wind, seismic, mammals, etc.) or manmade (due to ships, boat, harbor activities, aircraft just above the sea, etc.). Acoustic energy in water consists of molecular vibrations that travel at the speed of sound. The underwater acoustic channel is a time-varying frequency selective spatially uncorrelated channel with additive colored Gaussian noise.

EMD is a decomposition technique which considers the signal to have been consisting of various oscillatory modes and used for the time-frequency analysis of the signal. Researchers have proposed a fast EMD algorithm and identified that any signal can be decomposed into various stationary signals (Blakely, 2005). Boudraa (2007) proposed a signal filtering technique based on EMD in which a noisy signal is adaptively decomposed to intrinsic oscillatory signal. Delechelle *et al.* (2005) demonstrated

1 Corresponding author. E-mail: sakthivels@ssn.edu.in

that EMD acts essentially as a dyadic filter bank that can be compared with wavelet decomposition. They have also discussed on the mean envelope detection of the signal.

Lidar signals which are analogous to acoustic underwater signals are typical non-steady state, and non-stationary signals are difficult to be dealt with traditional filtering methods. Combination of EMD with Savitzky-Golay filter is proposed for denoising lidar echo signals that removes noise besides maintaining useful signal (Zhang *et al.*, 2010).

A non-linear time series analysis of a signal using EMD and Wavelet Decomposition (WD) has been presented by Wang *et al.* (2011) and inferred that EMD is better by determining the instantaneous balance position by acquiring the IMFs compared with WD. They have also identified that WD is better for analysis of linear signals where as EMD is better for both linear and non-linear analysis (Wang *et al*., 2011). Rilling and Flandrin (2008) investigated the EMD performance for a composite two tone signal and extended the analysis for non-linear model. The instantaneous frequency evolving with time is analyzed by the concept of Hilbert transform to the IMF signal is analyzed by Kim and Oh (2009). The drawback of applying HT on EMD in the presence of noise is analyzed and observed that the instantaneous frequency cannot be obtained for non-monochromatic IMF signals (Kasolvsky and Meyer). Application of EMD for biomedical applications considering white Gaussian noise for ECG is analyzed by a new methodology (Karagiannis and Constantinou, 2011).

2. Proposed EMD System

In general Hilbert transform is applied to the IMF signals derived from EMD to obtain the instantaneous frequency for colored Gaussian noises as shown in Fig. 1.

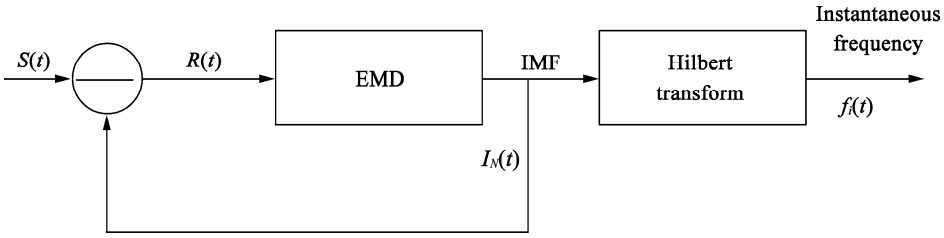

Fig. 1. EMD of stationary signal using Hilbert Transform.

In this paper, we have considered the analysis of an acoustic signal due to various ambient noises collected at depths of 5 m and 10 m from the sea surface. This signal is characterized as an additive colored Gaussian noise. In this case the obtained IMF is non-monochromatic and hence Hilbert spectrum analysis does not yield the extraction of the required signal. Hence a modification in the existing model is carried out by replacing Hilbert transform with Fourier Transform.

Fig. 2 shows the block diagram of the proposed algorithm in extraction of the reference signal transmitted by sonar against various ambient noises. For mathematical analysis, we consider a reference signal $r(t)$ combined with the non-stationary ambient noise signal $n(t)$ in the underwater channel and results in forming a noisy signal $S(t)$.

$$S(t) = r(t) + n(t) . \tag{1}$$

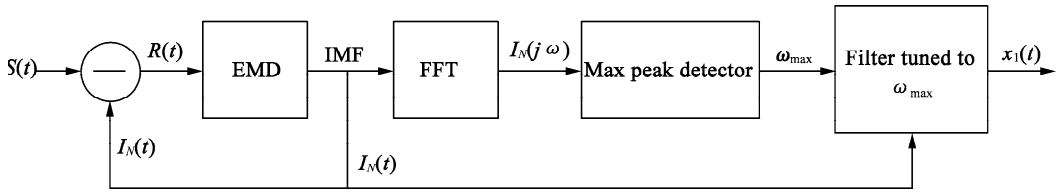

Fig. 2. Block diagram proposed model for extraction of stationary signal using EMD.

When EMD is applied to $S(t)$, its extrema points are calculated as follows:

$$Max = \text{Max}[S(t)]; \tag{2}$$

$$Min = \text{Min}[S(t)]. \tag{3}$$

The interpolation of *Max* and *Min* results in the upper and lower envelope of *S*(*t*) as given in Eqs. (4) and (5):

$$E_{\text{UE}}(t) = E_{\text{Upper Envelop}}(t) = \text{Interpolation}[Max]; \tag{4}$$

$$E_{\text{LE}}(t) = E_{\text{Lower Envelop}}(t) = \text{Interpolation}[Min]. \tag{5}$$

where, $E_{\text{Upper Envelop}}(t)$ is the upper envelope of the signal *S*(*t*), and $E_{\text{Lower Envelop}}(t)$ is the lower envelope of the signal *S*(*t*).

The mean *m*(*t*) of the received signal is calculated by averaging the upper and lower envelope,

$$m(t) = \frac{E_{\text{UE}}(t) + E_{\text{LE}}(t)}{2}. \tag{6}$$

Sifting process is carried out by eliminating the non-stationary components which result in $h_{k+1}(t)$.

$$h_{k+1}(t) = h_k(t) - m_k(t), \tag{7}$$

where, the detail signal in the first stage, $h_1(t) = S_1(t)$; $h_k(t)$ is the *k*-th stage detail in the sifting process; $m_k(t)$ is the *k*-th stage mean in the sifting process; and $h_{k+1}(t)$ is the *k*+1-th stage detail in the sifting process.

The detail signal is iterated till *m*(*t*) approaches zero. The final stage detail results in the formation of IMF signal $I(t)$. The residual signal $R(t)$ is obtained by subtracting $I(t)$ from $S(t)$. The iteration process is repeated until all available stationary signals are extracted and FFT is applied to the IMF to identify the dominant frequency.

Applying FFT to the *N*-th IMF results in

$$I_N(j\omega) = F[I_N(t)], \tag{8}$$

where $I_N(j\omega)$ is the frequency domain signal of *N*-th stage IMF.

The maximum peak detector identifies the frequency with the maximum amplitude $\omega_{\max}$ from $I_N(j\omega)$

$$I_N(j\omega_{\max}) = Max \cdot I_N(j\omega). \tag{9}$$

The narrow bandpass filter at the final stage tunes to the dominant frequency $\omega_{\max}$ resulting in the extraction of the dominant signal $F(\omega)$ available in that particular IMF as given in Eq. (10)

$$F(\omega) = I_N(\omega) \times H(\omega), \tag{10}$$

where, $F(\omega)$ is the frequency domain representation of the extracted signal, and $H(\omega)$ is the impulse response of narrow band pass filter tuned to $\omega_{\max}$.

This process of filtering is continued for all IMFs in order to obtain all the dominant signals available in the band of signal used for analysis. The reference signal $r(t)$ will be obtained as dominant signal in any of the IMFs depending upon the frequency of the signal used for analysis. Thus the proposed system identifies and extracts the required signal by eliminating all ambient noises in the underwater channel.

3. Proposed Algorithm

Step 1: Consider noisy acoustic signal $S(t)$, $S(t)=r(t)+n(t)$, where $r(t)$ is the reference signal and $n(t)$ is the noise signal;

Step 2: Identify all extrema points of $S(t)$;

Step 3: Compute $E_{\mathrm{UE}}(t)$ and $E_{\mathrm{LE}}(t)$ by interpolating *Max* and *Min*, respectively;

Step 4: Compute the mean, $m(t) = \dfrac{E_{\mathrm{UE}}(t) + E_{\mathrm{LE}}(t)}{2}$;

Step 5: Extract the detail, $h_{k+1}(t) = h_k(t) - m_k(t)$;

Step 6: Iterate on the residual signal $R(t)$;

Step 7: Repeat the above steps to obtain various modes of the noisy signal;

Step 8: Evaluate $I_N(j\omega) = F[I_N(t)]$ by applying FFT;

Step 9: Compute maximum frequency component, $I_N(j\omega_{\max}) = Max \cdot I_N(j\omega)$;

Step 10: Extraction dominant frequency by narrow band pass filteingr tunned to $\omega_{\max}$;

Step 11: Repeat the steps for all IMFs.

4. Results and Discussion

4.1 Data Collection

The data are collected at depths of 5 m and 10 m by use of Reson 4032 type of hydrophone at Bay of Bengal, Chennai for various wind speeds ranging from 2 to 6 m/s. The sampling frequency used for data collection is 50 kHz. The collected data comprises of noisy signal due to the signal generated by the Sonar (reference signal) and ambient noises (noise signal) because of various sources in the range from 100 Hz to 10 kHz.

Sifting Process:

The shifting process is carried out for $S(t)$, $E_{\mathrm{UE}}(t)$, $E_{\mathrm{LE}}(t)$ and $m(t)$ for 24 iterations and its results for iterations 1, 2, 3, 5, 10, 12, 15, 16, 18, and 21 are shown in Fig. 3. The amplitude of $r(t)$

considered is very minimal compared with $n(t)$.

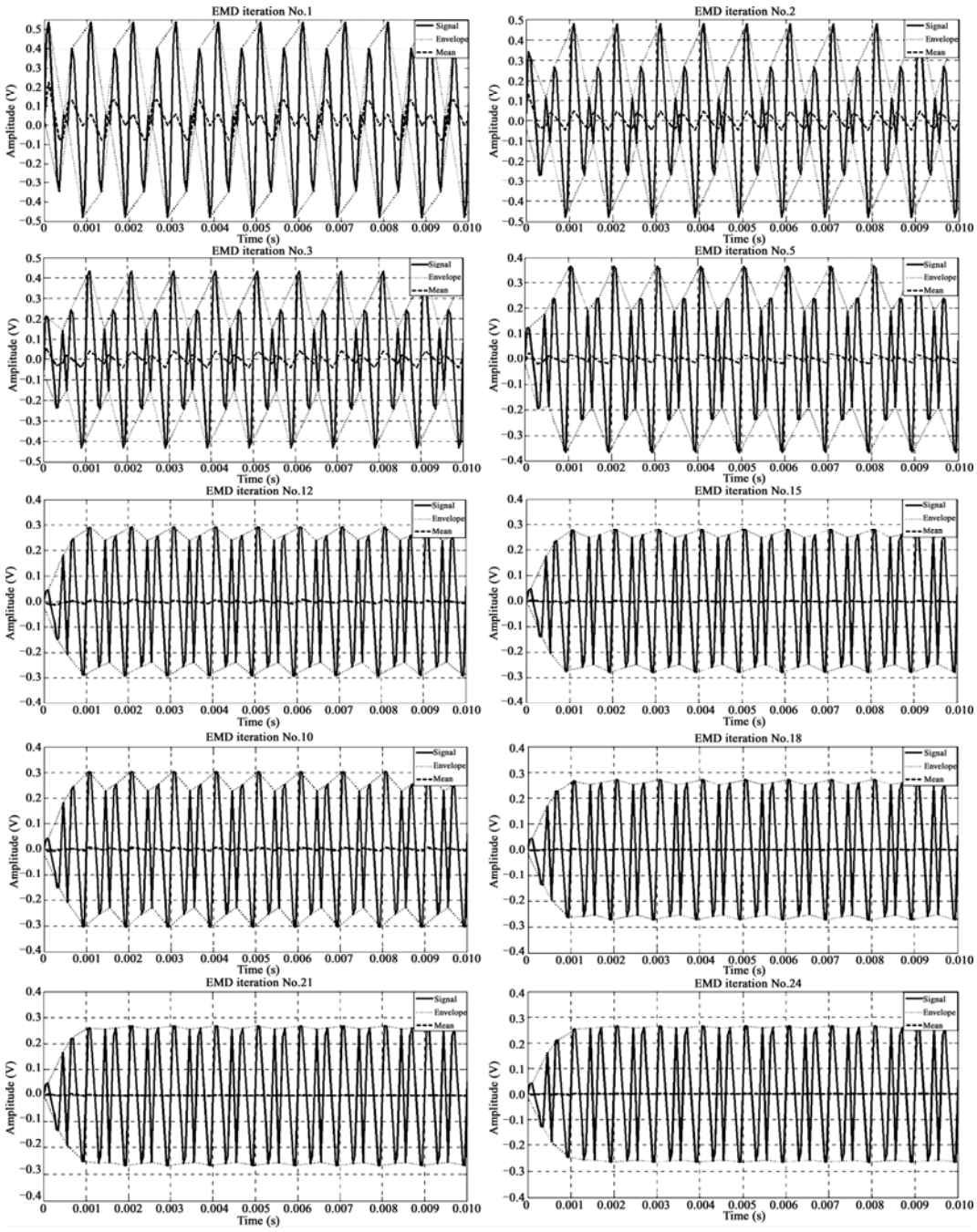

Fig. 3. Sifting process.

It can be observed that at initial stage there is the maximum variation in the envelope. The

difference between $n(t)$ and $m(t)$ is fed as input for the next iteration. The above process is repeated until $m(t)$ approaches to zero (approximately) as further iterations will not result in smoothening. Thus the stationary periodic signal is extracted from the non-stationary signal.

4.2 Extraction of Stationary Signal from Non-Stationary Noisy Signal by Single IMF

When the ambient noise $n(t)$ combines with $r(t)$, $S(t)$ becomes a non-linear non-stationary signal. From $S(t)$, stationary components $I(t)$ are extracted by IMF as shown in Fig. 4. After removing $I(t)$ from $S(t)$, the resultant called residual signal $R(t)$ is fed for the next iteration.

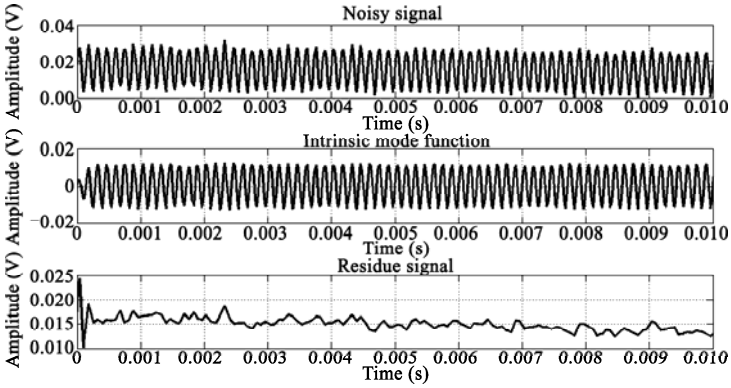

Fig. 4. Noisy signal, IMF and residual signal in time domain.

The above process is repeated till the last periodic component is extracted from $R(t)$. $R(t)$ and $I(t)$ for eight stages is shown in Fig. 5.

From Fig. 5, we can observe that four different periodic signals are extracted in the first four stages of IMF from the random $R(t)$. Further, the non-existence of periodic signals after four stages of IMF is identified. Hence, it can be concluded that based on $R(t)$, the different periodic signals can be extracted within few stages of IMF. Furthermore, after four stages of IMF only non-periodic signals is extracted from $R(t)$ which clearly shows the non-availability of the desired periodic signals.

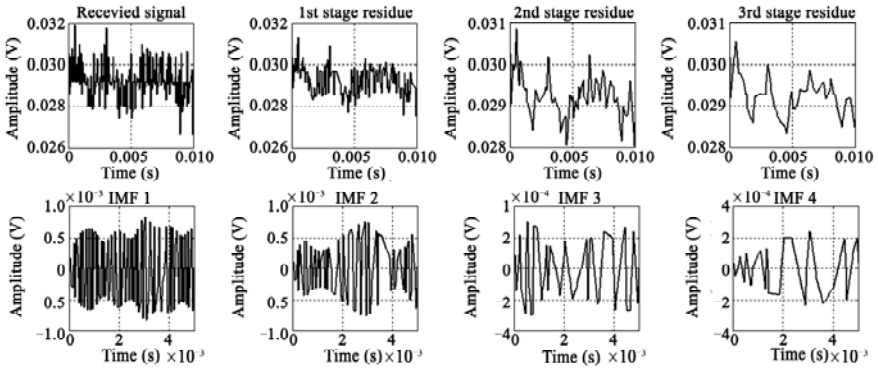

Fig. 5a. Time domain analysis of various modes.

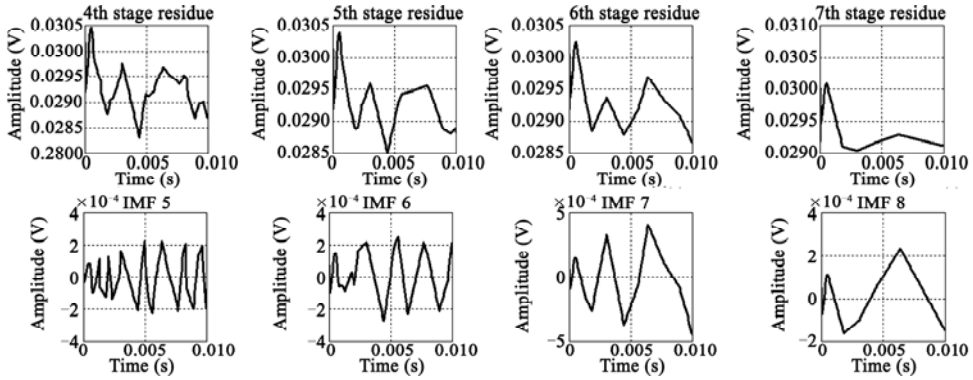

Fig. 5b. Time domain analysis of various modes.

4.3 Spectral Analysis of the Periodic Signals Extracted by IMF

In order to validate the proposed algorithm, we consider a reference signal of 500 Hz. The spectral analysis of the extracted signal using IMF is shown in Fig. 6 from which we infer that the $R(t)$ does not show any peak at 500 Hz. In contrast, after IMF processing we are able to extract the periodic signals contained in $R(t)$ at 500 Hz, 1 kHz, 2 kHz and 5.7 kHz.

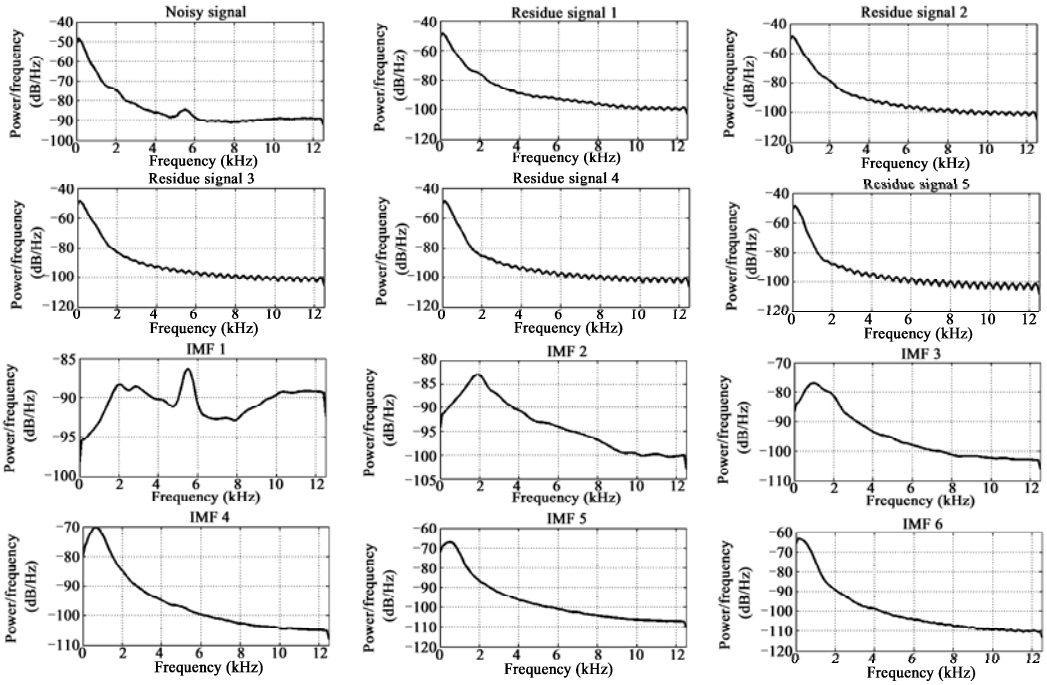

Fig. 6. Power spectral analysis of specified data.

In the above extracted frequencies 1 kHz, 2 kHz and 5.7 kHz are due to some other sources in the underwater channel which may be due to ambient noise. From this we strongly conclude that EMD sifting process is capable of identifying all the periodic signals in the underwater channel.

Next we consider two noisy signals, in which one noisy signal contains a known input reference of 2.5 kHz. From Fig. 7 we can observe that the PSD of the two noisy signals overlaps in amplitude. After applying EMD, IMF 1 clearly identifies the availability of 2.5 kHz reference signal in one of the noisy signals. After extracting 2.5 kHz reference signal, it can be observed that the correlation between both the noisy signals is the maximum from IMF 2 to IMF 6. Hence it is evident that even a very low amplitude acoustic signal corrupted by ambient noises can be easily identified and extracted.

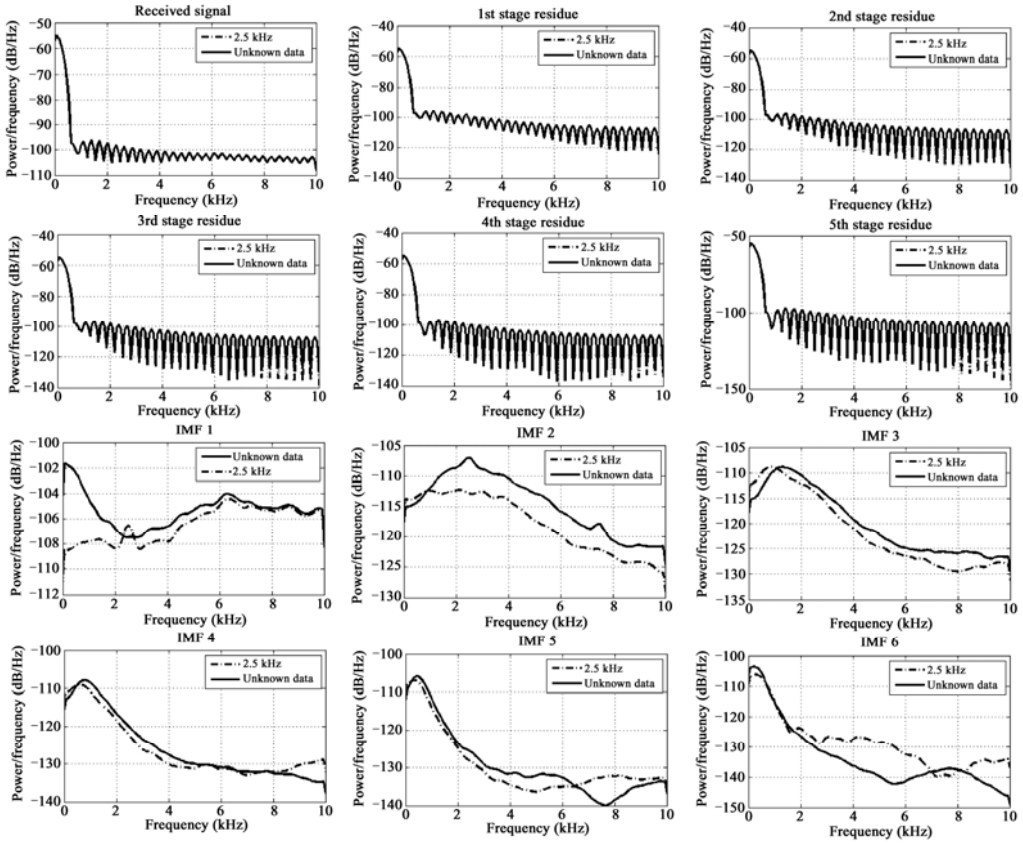

Fig. 7. Comparison of data with and without reference signal.

In order to further evaluate, we consider $r(t)$ of 7 kHz buried in $n(t)$ forming $S(t)$. The time and frequency domain of $r(t)$, $n(t)$, and $S(t)$ signals are shown in Figs. 8 and 9.

By applying EMD, the time and frequency domain of the four stages of IMF are shown in Figs. 10 and 11. The time domain represents the presence of periodic signals along with noises. The FFT in Fig. 11 clearly shows the presence of reference signals at various IMFs. It can be observed that the high frequency signal (7 kHz) that is dominant is identified in IMF 1. The other frequencies that are dominant are subsequently identified in the later stages of IMF.

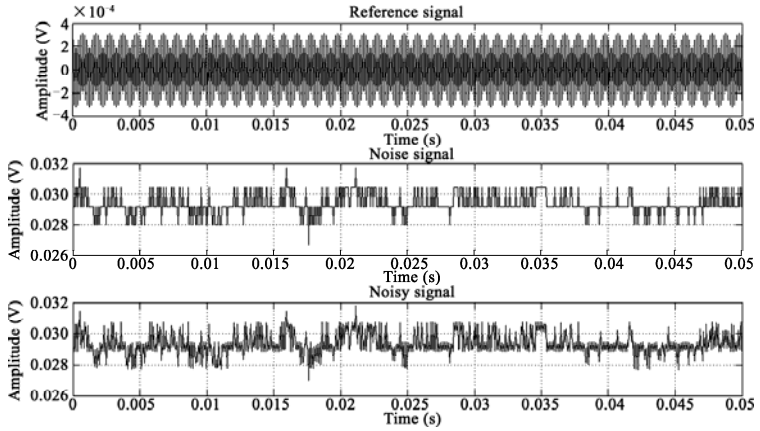

Fig. 8. Time domain analysis of reference signal $r(t)$, noise $n(t)$ and noisy signal $S(t)$.

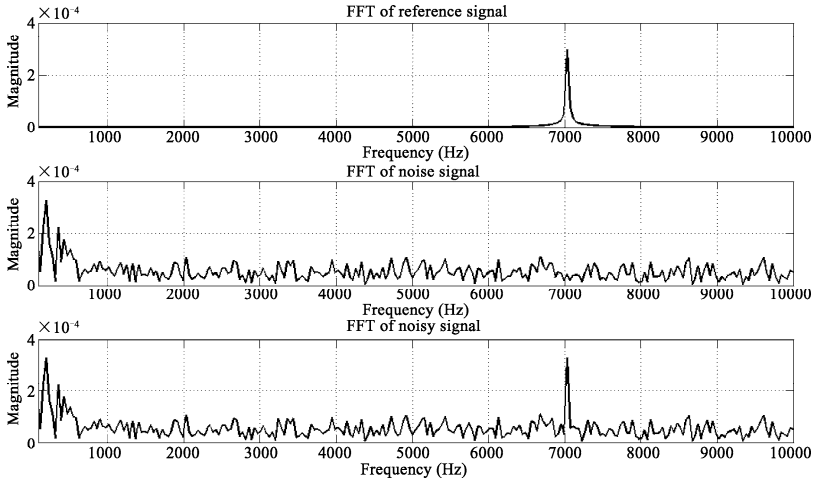

Fig. 9. FFT of reference signal $r(t)$, noise $n(t)$ and noisy signal $S(t)$.

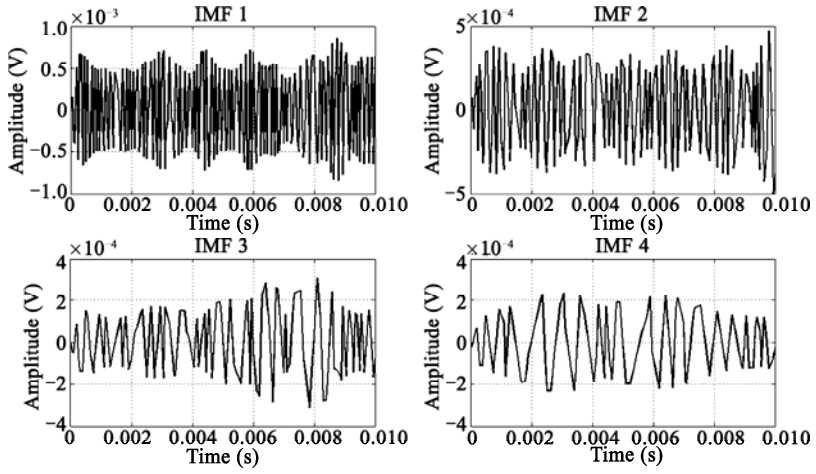

Fig. 10. Time analysis of intrinsic mode function.

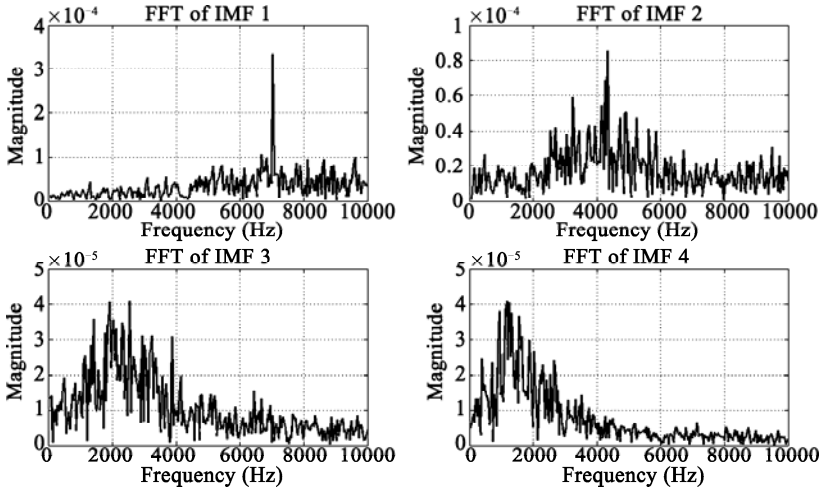

Fig. 11. FFT of intrinsic mode function.

The dominant signals identified at each IMF stage is extracted by a narrow bandpass filter tunned to ω_{max}. From Figs. 12 and 13, it is evident that the reference signal (7 kHz) is extracted. It is also inferred that the noise data considered for analysis contain a signal at 4.2 kHz in IMF 2 which is also identified and extracted along with 2.4 kHz and 1 kHz in IMF 3 and IMF 4. These frequencies may be due to some sources in the underwater channel.

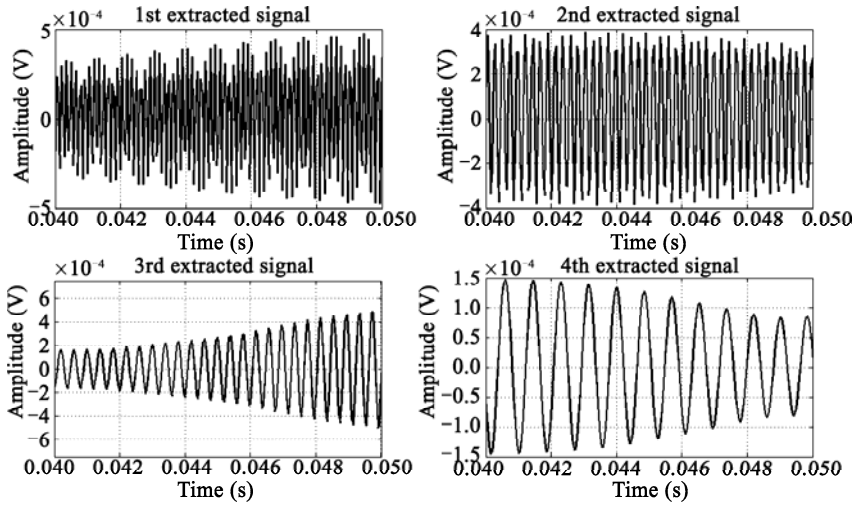

Fig. 12. Time domain of extracted acoustic signal.

4.4 SNR Analysis

SNR is an important performance metric for evaluating any system's performance. We analyze the output SNR for the following cases:

Case 1: High frequency reference signals ranging from 5 kHz to 9 kHz.

Case 2: Low frequency reference signals ranging from 500 Hz to 4 kHz.

Case 3: Various wind speeds ranging from 2 m/s to 6.57 m/s.

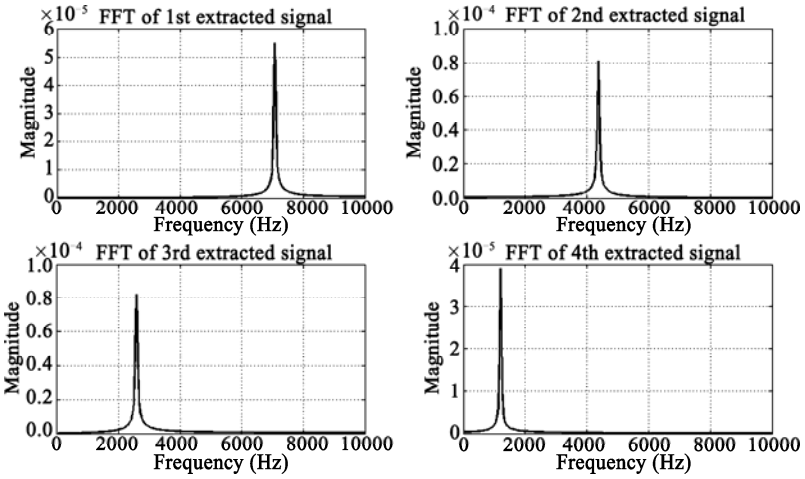

Fig. 13. FFT of extracted acoustic signal.

Case 1: High Frequency Reference Signals Ranging from 5 kHz to 9 kHz

The performance of the proposed EMD algorithm for a high frequency sonar generated input signals ranging from 5 kHz to 9 kHz transmitted in underwater channel against wind driven ambient noise at a wind speed of 2 m/s is shown in Fig 14. The performance is evaluated for an input SNR ranging from −10 dB to 10 dB for a 5 kHz input signal. It is observed that output SNR increases to 39.03 dB for an input SNR of −10 dB and to 48.95 dB for an input SNR of 10 dB. Similarly, for 7 kHz and 9 kHz signals, the output SNR increases from 38.57 dB to 45.95 dB and 37.91 dB to 43.03 dB, respectively.

Further, from Fig. 14 we can observe that the output SNR improvement is appreciable for very high input SNR compared with low input SNR. Table 1 summarizes the output SNR for various frequencies.

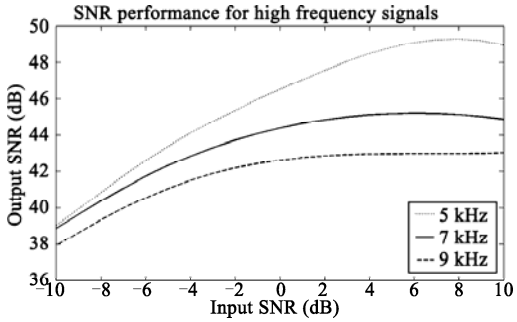

Fig. 14. SNR performance for high frequency input signals ranging from 5 kHz to 9 kHz.

Table 1 SNR improvement for high frequency input acoustic signals

Frequency of reference signal (kHz)	0.5	7	8	9
Input SNR(dB)	Output SNR(dB)			
−10	39.03	38.57	38.87	37.91
−5	43.38	42.38	42.32	41.06
0	46.50	44.77	44.37	42.62
5	48.81	45.58	45.18	42.97
10	48.95	45.95	44.87	43.03

Case 2: Low Frequency Reference Signals Ranging from 500 Hz to 4 kHz

Fig. 15 illustrates the performance for low frequency acoustic signals ranging from 500 Hz to 4 kHz transmitted in underwater channel against wind driven ambient noise with a wind speed of 2 m/s. The performance is evaluated for an input signal of 500 Hz, 2 kHz and 4 kHz with the input SNR ranging from −10 dB to 10 dB. It can be seen that for an input SNR of −10 dB, output SNR increases to −2.23 dB, 27.64 dB and 41.67 dB for 500 Hz, 2 kHz and 4 kHz, respectively. Similarly for 10 dB input SNR, the output SNR improves to 27.07, 39.68 dB and 47.32 dB.

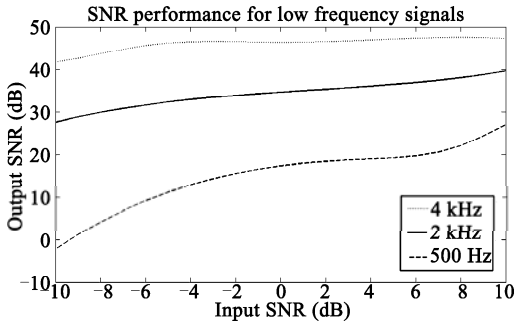

Fig. 15. SNR performance for low frequency input signals ranging from 500 Hz to 4 kHz.

Further, from Fig. 15 we can observe that the EMD-based approach results in better output SNR improvement even in the presence of dominant wind noise at lower frequencies. The output SNR achieved for various input frequencies of 0.5, 1, 2 and 4 kHz are shown in Table 2.

Table 2 SNR improvement for low frequency input acoustic signals

Frequency of reference signal (kHz)	0.5	1	2	3	4
Input SNR(dB)	Output SNR(dB)				
−10	−2.235	17.63	27.64	27.87	41.67
−5	11.25	18.73	32.35	32.76	46.27
0	17.38	25.92	34.71	37.54	46.41
5	19.25	27.74	36.54	41.38	47.19
10	27.07	27.99	39.68	42.87	47.32

Case 3: Various Wind Speeds Ranging from 2.11 m/s to 6.57 m/s

The SNR improvement performance of the proposed EMD based algorithm for various wind speeds data ranging from 2.11 m/s to 6.57 m/s is shown in Fig. 16. It is observed that the SNR improvement is less at higher wind speed compared with lower wind speeds. It is because the wind driven ambient noise will be predominant in the case of higher wind speed and hence resulting in poor SNR improvement. The output SNR achieved for various wind speeds are shown in Table 3.

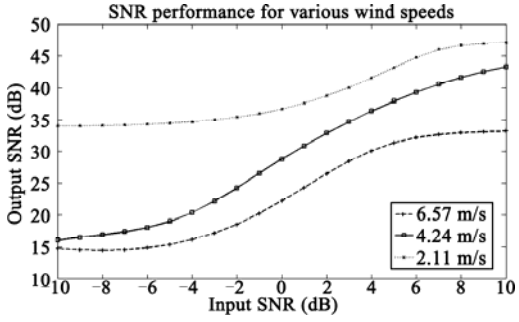

Fig. 16. SNR performance for various wind speeds.

Table 3 SNR improvement for various wind speeds

Wind speed (m/s)	2.11	3.32	4.24	5.92	6.57
Input SNR(dB)	Output SNR(dB)				
−10	34.02	32.98	16.02	22.37	14.72
−5	34.49	34.25	18.99	23.99	15.33
0	36.72	35.97	28.74	25.06	22.19
5	43.22	40.79	37.76	30.64	31.35
10	47.08	46.70	43.35	36.20	33.24

5. Conclusion

In the present study, we evaluate the performance of the proposed algorithm based on EMD for identification and extraction of desired sonar signals buried in underwater ambient noises. Our analysis clearly shows that the proposed algorithm results in better identification of the reference signal against noises in the underwater channel. Simulation results confirm that in addition to the extraction of the known reference signal, the algorithm can also extract other periodic signal components embedded in the underwater residual signals. We also observe that the SNR improvement is better for low frequency reference signals.

Acknowledgements − The authors wish to thank Dr. S. Radha HOD/ECE department, SSNCE along with Mr. B. Lakshmi Narayanan, and Mr. J. Mohamed Meerasahib (UG students) for their support.

References

Blakely, C. D., 2005. *A Fast Empirical Mode Decomposition Technique for Nonstationary Nonlinear Time Series*, Center for Scientific Computation and Mathematical Modeling, University of Maryland, College Park MD 20740 USA, Elsevier Science 3rd Ed., 1–14.

Boudraa, A. O., 2007. EMD based signal filtering, *IEEE Transactions on Instrumentations and Measurements*, **56**(6): 2196–2202.

Delechelle, E., Lemonie, J. and Niang, O., 2005. Empirical mode decomposition: An analytical approach for sifting process, *IEEE Signal Processing Letters*, **12**(11): 764–767.

Karagiannis, A. and Constantinou, P., 2011. Noise-assisted data processing with empirical mode decomposition in biomedical signals, *IEEE Transactions on Information Technology in Biomedicine*, **15**(1): 11–18.

Kasolvsky, D. N. and Meyer, F. G., 2010. Noise corruption of empirical mode decomposition and its effect on instantaneous frequency, *Advances in Adaptive Data Analysis*, **2**(3): 376–393.

Kim, D. and Oh, H. S., 2009. EMD: A package for empirical mode decomposition and Hilbert spectrum, *The R Journal*, **1**(1): 40–46.

Rilling, G. and Flandrin, P., 2008. One or two frequencies the empirical mode decomposition answers, *IEEE Transactions on Signal Processing*, **56**(1): 85–95.

Wang, X. J., Feng, G. L. and Feng, A. X., 2011. On performance difference of EMD and WD in the nonlinear time series analysis, *Proceedings of the Eighth International Conference on Fuzzy Systems and Knowledge Discovery* (*FSKD*), **1**, 207–211.

Zhang, Y. K., Ma, X. C., Hua, D. X., Cui, Y. A. and Sui, L. S., 2010. An EMD-based denoising method for Lidar Signal, *Proceedings of the 3rd International Congress on Image and Signal Processing*, **8**, 4016–4019.